Mid-Wavelength Infrared Responsivity of Colloidal Quantum Dot/Organic Hybrid Photodetectors

ECS Transactions, 97 (1) 109-115 (2020)
10.1149/09701.0109ecst ©The Electrochemical Society

Mid-Wavelength Infrared Responsivity of Colloidal Quantum Dot/Organic Hybrid Photodetectors

Shihab Bin Hafiz[a], Mohammad Mostafa Al Mahfuz[a], and Dong-Kyun Ko[a]

[a] Department of Electrical and Computer Engineering, New Jersey Institute of Technology, Newark, New Jersey 07102, USA

Colloidal quantum dot/organic hybrid materials approach offer a path toward engineering solution-processed photodetectors with extended spectral responsivity in the infrared. We demonstrate this approach in the technologically important thermal infrared region of mid-wavelength infrared, utilizing a solution blend of Ag_2Se colloidal quantum dots and [6,6]-phenyl-C_{61}-butyric acid methyl ester (PCBM). We report on the device fabrication and their optical, electrical, and optoelectronic properties. At room temperature, a responsivity of 0.2 mA/W was measured under 5 μm irradiation and 5 V bias. The new hybrid optoelectronic film demonstrated in this study brings the advantage of cost-effectiveness and greater fabrication versatility than the single crystal or epitaxial semiconductors that comprise today's infrared technologies.

Introduction

Photodetectors exhibiting high sensitivity have been the hallmark of colloidal quantum dot (CQD)-based optoelectronics. Specifically, films composed of PbS CQDs have been reported to show a detectivity of 10^{13} Jones in the short-wavelength infrared (1) and recently, CdTe CQDs have been utilized to fabricate visible photodetectors with detectivity reaching 10^{17} Jones, owing to high gain (2). An alternate approach to designing solution-processed photoconductive devices is to utilize organic/inorganic hybrids (3). In these devices, inorganic CQDs, which are the photoactive elements, are homogeneously embedded in an organic matrix that serve as a charge transporting medium. Upon illumination, photoexcited holes (electrons) are transferred to the organic hole (electron) transporting material (4), which are then collected at the electrode. These hybrid photoconductors have been studied previously in the limited spectral ranges in the infrared (3) while extending the photoresponse toward the longer wavelengths would have great implications in terms of their applications.

In this work, we report the fabrication and characterization of mid-wavelength infrared (MWIR = 3 – 5 μm) photodetectors based on [6,6]-phenyl-C_{61}-butyric acid methyl ester (PCBM) and Ag_2Se CQD blends. The Ag_2Se CQDs are newly emerging, heavy metal-free colloidal nanomaterial that exhibits tunable optical absorption in MWIR via intraband (intersubband) optical transition (5,6). We chose PCBM as an electron transporting matrix material due to minimal molecular vibration signatures in the 3-5 μm region (7) and its high carrier mobility than the conjugated polymers. Also, our devices do not need the ligand exchange process which is typically required for CQD film-based

devices. We note that this is of significant advantage since the strength of intraband optical absorption of Ag_2Se CQD is heavily dependent on the concentration of excess electrons present in a CQD, which is typically reduced after the ligand exchange due to de-doping effect (5,8). In addition, the hybrid approach presented herein may serve as a promising strategy to minimizing the dark current in devices utilizing highly-doped intraband CQDs.

Experiments

Ag_2Se CQD Synthesis

Ag_2Se CQDs having MWIR absorption peak centered at 4.94 μm were synthesized by modifying the previously reported procedure (5). Briefly, 15 mL of oleylamine was added to a three-neck flask and the temperature was raised to 80 °C for 1 hour under vacuum. Meanwhile, 1 M TOP-Se and 0.5 M TOP-Ag were prepared though dissolving Se powder and AgCl in trioctylphosphine (TOP), respectively, inside the glovebox. After switching the atmosphere to nitrogen, 2 mL of 1.0 M TOP-Se was added to oleylamine and the temperature of the mixture was increased to 170 °C. Then, 2 mL of 0.5 M TOP-Ag was swiftly injected which was followed by a quick color change of the mixture to dark brown. The reaction was quenched after 5 seconds by injecting 10 mL of butanol and cooling using a water bath. The CQDs were then precipitated with a mixture of ethanol and methanol. After centrifugation, the final precipitate was redispersed in chlorobenzene after two methanol washes.

Hybrid PCBM/Ag_2Se CQD Film Deposition

PCBM solution was first prepared by dissolving 8 mg of PCBM in 0.5 mL of chlorobenzene. In a separate vial, Ag_2Se CQD solution was prepared by dissolving 12 mg of Ag_2Se CQD powder in 0.5 mL of chlorobenzene. Both were blended to create 1 mL of hybrid solution with a Ag_2Se CQD : PCBM weight ratio of 1.5 : 1. The amount of Ag_2Se CQDs was adjusted to prepare other hybrid solutions with varying weight ratios. The films for both optical characterization and devices were deposited using spin-casting at 1000 rpm for 40 seconds, followed by annealing at 70 °C for 1 hour. The film thickness was in the range of 50 – 100 nm.

Optical Absorbance Characterization

Hybrid and pure PCBM films were deposited onto ZnSe disc, following the procedure described above. The absorption spectra were obtained using Thermo Nicolet Avatar 370 FTIR spectrometer in transmission configuration.

Device Fabrication and Measurements

Photoconductive photodetector devices were fabricated by depositing hybrid or pure PCBM film onto Si/SiO_2 substrates with pre-patterned interdigitated electrodes (Cr/Au). The channel length and width were 10 μm and 64.9 mm, respectively. A calibrated blackbody (Newport 67030, 900 °C) coupled with 5 μm bandpass filter was used as an

illumination source. The current was measured using Agilent 4155A semiconductor parameter analyzer.

Results and Discussion

We first performed optical characterizations of colloidal quantum dot/organic hybrid blend to examine the prospect for MWIR optoelectronics. Figure 1 shows the Fourier transform infrared (FTIR) spectra obtained from pure PCBM, Ag_2Se CQD, hybrid PCBM/Ag_2Se CQD films. The film composed of pure PCBM (Figure 1a) shows characteristic peaks around 5.7, 7.0, and 8.7 μm (denoted with star symbol), which arise from the vibrational signatures of carbon to oxygen (C=O) double bonds, CH_2 bending, and oxygen to carbon (O–C) single bonds, respectively (7). The absence of significant molecular absorptions in the MWIR makes PCBM a good candidate for near-transparent/electron-transporting medium. On the other hand, Ag_2Se CQDs (Figure 1b) exhibit a strong MWIR intraband absorption peak centered at 4.94 μm, which can be used as MWIR photoactive elements. The hybrid films (Figure 1c, Ag_2Se CQD : PCBM weight ratio = 15 : 1) shows the sum of both components where, on top of underlying PCBM molecular absorbance, MWIR absorption arising from Ag_2Se CQDs is still prominent.

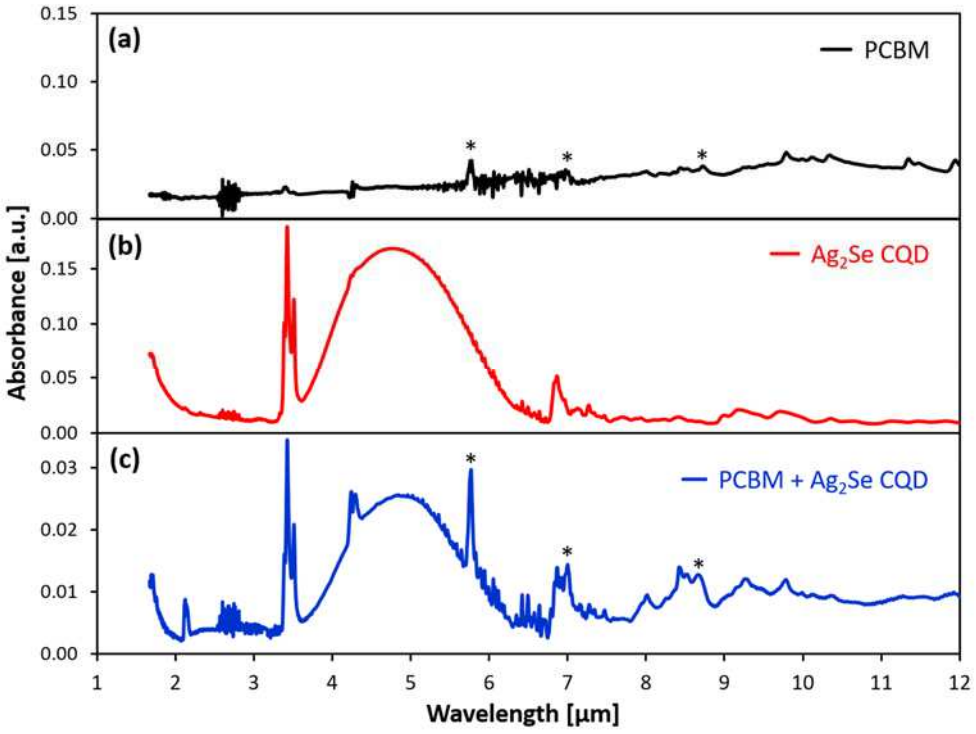

Figure 1. Optical absorbance characterization of (a) pure PCBM, (b) Ag_2Se CQD, and (c) hybrid PCBM/Ag_2Se CQD films. Star symbols denote characteristic peaks of PCBM which arise from the vibrational signatures of carbon to oxygen double bonds (~5.7 μm), CH_2 bending (~7.0 μm), and oxygen to carbon single bonds (~8.7 μm).

Along with the suitable optical properties, energy level alignment between the PCBM and Ag_2Se CQDs are critical in realizing functional devices. Energy levels of PCBM (9)

and Ag_2Se CQD (10) has been previously measured using photoelectron spectroscopy and are plotted in Figure 2(a). After the formation of a hybrid film, an expanded view of conduction energy levels, which govern the transport of electrons, is shown in Figure 2(b). Under 5 μm MWIR irradiation, electrons occupying the first quantum-confined conduction energy level ($1S_e$) of Ag_2Se CQD is expected to photoexcite to the second quantum-confined conduction energy level ($1P_e$). Under bias, these photocarriers will be injected into the electron transporting PCBM through field emission and contribute to the photocurrent (4), as shown in Figure 2(c).

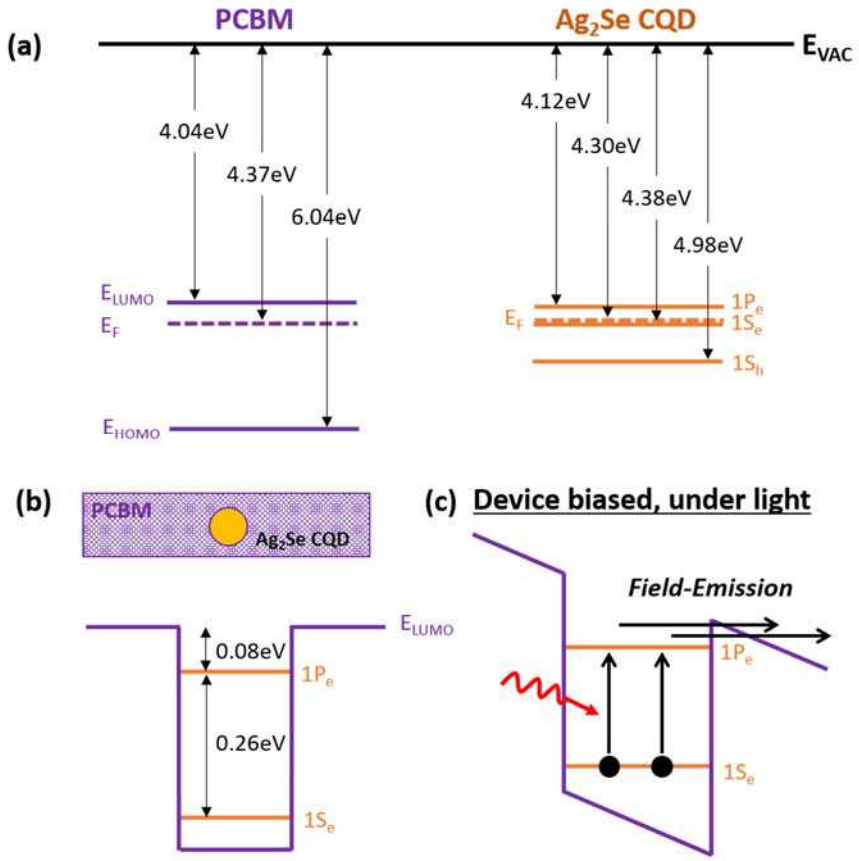

Figure 2. Schematic illustration of (a) energy level alignment between PCBM and Ag_2Se CQD. E_{LUMO}, E_{HOMO}, E_F, $1S_h$, $1S_e$, and $1P_e$ denote lowest unoccupied molecular orbital of PCBM, highest occupied molecular orbital of PCBM, Fermi energy level, first quantum-confined valence energy level of Ag_2Se CQD, first quantum-confined conduction energy level of Ag_2Se CQD, and second quantum-confined conduction energy level of Ag_2Se CQD, respectively. (b) depicts an expanded view of conduction energy levels of hybrid blend and (c) conduction energy levels under bias and light.

Hybrid films with different Ag_2Se CQD : PCBM weight ratios, varying from 15 : 1 to 0.015 : 1, have been prepared to fabricate photoconductive photodetectors. Figure 3a shows a solution containing PCBM and Ag_2Se CQD blend (1.5 : 1). Transmission electron microscopy (TEM) images taken from hybrid films show a random, homogeneous distribution of Ag_2Se CQDs in PCBM with no observable phase segregation. The dark resistivity of the film has been measured as a function of Ag_2Se CQD loading, as shown in Figure 3c. Interestingly, we observe that the resistivity reduces

with increasing CQD loading. The introduction of Ag_2Se CQDs inside PCBM would inhibit the transport of electron rather than enhancing it thus, the reduction in resistivity is expected to arise from the increase in electron concentration. While the increase in the majority carrier concentration with increasing CQD loading has been previously attributed to the interfacial charge separation of thermal carriers in TESAN-BT/CdSe CQD hybrids (11), more study is required to confirm the mechanism in our hybrid system.

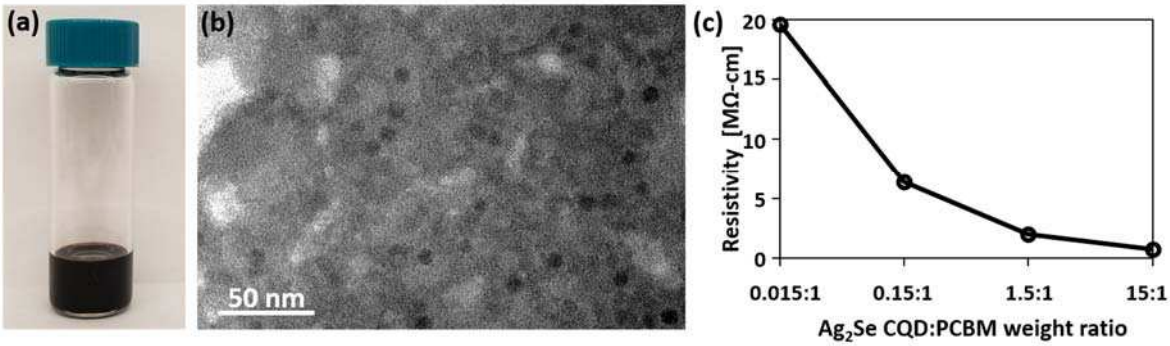

Figure 3. Photograph of (a) solution blend of PCBM/Ag_2Se CQD, (b) TEM image of as-deposited hybrid film, and (c) dark resistivity vs. Ag_2Se CQD loading plot.

Figure 4 shows the photoconductivity measurement obtained from films with increasing Ag_2Se CQD loading. While pure PCBM shows no change in the current before and after 5 μm irradiation (Figure 4a), introduction of Ag_2Se CQDs in PCBM (Ag_2Se CQD : PCBM weight ratio = 0.75 : 1) induce observable changes in the current after irradiation (Figure 4b). Increasing the CQD loading further to 7.5 : 1 increases the magnitude of the response, as shown in Figure 4c. A close examination of Figure 4c data reveals two distinct temporal features: a sharp initial increase in the current followed by a slow saturating current. We assign the initial rapid change in the current as a response arising from optoelectronic effect (excess carrier generation through photoexcitation) and a slow saturating current as a response arising from thermal/bolometric effect (increased thermal population of carriers due to rise in temperature). Estimating the photocurrent solely from the optoelectronic contribution, the responsivity is calculated to be 0.2 mA/W (5 V bias) for 7.5 : 1 hybrid film. It is interesting to note that while pure PCBM shows no thermal/bolometric effect, the addition of Ag_2Se CQDs causes the thermal/bolometric effect to occur. The magnitude of the thermal/bolometric response also increases with increasing Ag_2Se CQD loading. Based on our measurement that 5 μm irradiation (optical power = 32.32 μW) gives approximately 1 °C increase in the device temperature, temperature coefficient of resistance (TCR) is estimated to be -1.8 $\%K^{-1}$ for 0.75 : 1 hybrid, which increases to -3.1 $\%K^{-1}$ for 7.5 : 1 hybrid films. Overall, incorporation of Ag_2Se CQD not only give rise to 5 μm optoeletronic response but also induce thermal/bolometric response. Further studies are on the way to elucidate the mechanism of CQD-induced thermal effect.

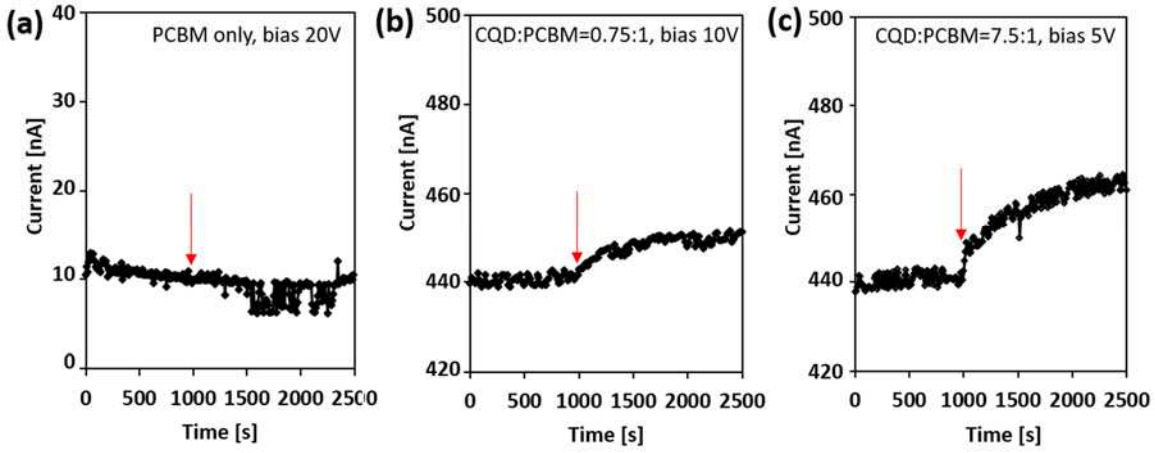

Figure 4. Photoconductivity measurement of (a) pure PCBM, (b) hybrid with Ag_2Se CQD : PCBM weight ratio = 0.75 : 1, and (c) hybrid with 7.5 : 1 weight ratio. Red arrows denote when the irradiation was on.

Conclusion

In summary, we have investigated the optical and electrical properties of PCBM/Ag_2Se CQD organic/inorganic hybrid films and fabricated photoconductive photodetectors to test the feasibility of MWIR detection. Both optoelectronic and thermal effects contribute to the 5 μm MWIR current response. The responsivity arising from optoelectronic effect was estimated to be 0.2 mA/W (room temperature, 5 V bias) while further optimizing Ag_2Se CQD concentration and film thickness could lead to higher values. The new hybrid film demonstrated in this study may open up many opportunities for low-cost optoelectronics in the MWIR where solution-processed material options are rare.

Acknowledgments

This work was supported by National Science Foundation Grant No. ECCS-1809112.

References

1. G. Konstantatos, I. Howard, A. Fischer, S. Hoogland, J. Clifford, E. Klem, L. Levina and E. H. Sargent, *Nature*, **442**, 180–183 (2006).
2. Y. Zhang, D. J. Hellebusch, N. D. Bronstein, C. Ko, D. F. Ogletree, M. Salmeron and A. P. Alivisatos, *Nat. Comm.*, **7**, 11924 (2016).
3. R. Saran and R. J. Curry, *Nat. Photon*ics, **10**, 81–92 (2016).
4. A. D. Stiff-Roberts, K. R. Lantz and R. Pate, *J. Phys. D Appl. Phys.,* **42**, 234004 (2009).
5. S. Hafiz, M. R. Scimeca, P. Zhao, I. J. Paredes, A. Sahu and D. -K. Ko, *ACS Appl. Nano Mater.*, **2**, 1631-1636(2019).
6. S. B. Hafiz, M. R. Scimeca, A. Sahu, and D.-K. Ko, *ECS Trans.*, **92**(1), 11-16 (2019).

7. S. –A. Gopalan, M. –H. Seo, G. Anantha-Iyengar, B. Han, S. –W. Lee, D. –H. Kwon, S. –H. Lee and S. –W. Kang, *J. Mater. Chem. A*, **2**, 2174 (2014).
8. A. Robin, C. Livache, S. Ithurria, E. Lacaze, B. Dubertret, and E. Lhuillier, *ACS Appl. Mater. Interfaces*, **8**, 27122– 27128 (2016).
9. J. Maibach, E. Mankel, T. Mayer and W. Jaegermann, *J. Mater. Chem. C*, **1**, 7635-7642 (2013).
10. J. Qu, N. Goubet, C. Livache, B. Martinez, D. Amelot, C. Gréboval, A. Chu, J. Ramade, H. Cruguel, S. Ithurria, M. G. Silly, and E. Lhuillier, *J. Phys. Chem. C*, **122**, 18161-18167 (2018).
11. D. S. Chung, Y. –H. Kim and J. –S. Lee, *Nanotechnology*, **25**, 035202 (2013).